Development 139, 4123-4132 (2012) doi:10.1242/dev.083006

Endogenous Nodal signaling regulates germ cell potency during mammalian testis development

Cassy M. Spiller[1], Chun-Wei Feng[1], Andrew Jackson[1], Ad J. M. Gillis[2], Antoine D. Rolland[1], Leendert H. J. Looijenga[2], Peter Koopman[1,*] and Josephine Bowles[1]

SUMMARY

Germ cells, the embryonic precursors of sperm or oocytes, respond to molecular cues that regulate their sex-specific development in the fetal gonads. In males in particular, the balance between continued proliferation and cell fate commitment is crucial: defects in proliferation result in insufficient spermatogonial stem cells for fertility, but escape from commitment and prolonged pluripotency can cause testicular germ cell tumors. However, the factors that regulate this balance remain unidentified. Here, we show that signaling by the TGFβ morphogen Nodal and its co-receptor Cripto is active during a crucial window of male germ cell development. The Nodal pathway is triggered when somatic signals, including FGF9, induce testicular germ cells to upregulate *Cripto*. Germ cells of mutant mice with compromised Nodal signaling showed premature differentiation, reduced pluripotency marker expression and a reduced ability to form embryonic germ (EG) cell colonies in vitro. Conversely, human testicular tumors showed upregulation of *NODAL* and *CRIPTO* that was proportional to invasiveness and to the number of malignant cells. Thus, Nodal signaling provides a molecular control mechanism that regulates male germ cell potency in normal development and testicular cancer.

KEY WORDS: Nodal, Germ cell, Pluripotency, Mouse

INTRODUCTION

Germ cells in the mouse fetal gonad are normally exposed to molecular signals from the soma that trigger their differentiation into sperm or oocytes (McLaren, 1983). In an ovary, germ cells enter meiosis and commit to oogenesis around 13.5 days post coitum (dpc) (Monk and McLaren, 1981; Speed, 1982). Recent studies have demonstrated that retinoic acid (RA) present in the ovary triggers germ cell entry into meiosis. In a testicular environment, RA is prevented from inducing meiosis by the action of the degradative p450 enzyme CYP26B1 (Bowles et al., 2006; Koubova et al., 2006). Fibroblast growth factor 9 (FGF9) becomes upregulated following the expression of SRY and SOX9 in the pre-Sertoli cells of the developing testis. In addition to its important functions in regulating somatic cell differentiation in the developing testis (Colvin et al., 2001), FGF9 actively suppresses entry into meiosis and stimulates commitment to spermatogenesis in the germ cell lineage (Barrios et al., 2010; Bowles et al., 2010). During normal development, testicular germ cells maintain expression of pluripotency markers, including *Oct4* and *Sox2*, for about 2 days longer than XX germ cells, then cease dividing and upregulate expression of male fate marker genes, including *Nanos2* (Tsuda et al., 2003). Although the transition from pluripotency to differentiation in the period 12.5-14.5 dpc is a crucial stage in the development of male fetal germ cells, it is not known how this transition is regulated at the molecular level.

Germ cells are often considered differentiated, uni-potential cells because they usually generate only gametes. However, during some phases of fetal life they are able to revert to functional pluripotency both in vitro and in vivo. Germ cells isolated between 8.0 and 13.5 days post coitum (dpc) and cultured in a combination of stem cell factor (SCF), leukemia inhibitory factor (LIF) and basic fibroblast growth factor (bFGF, FGF2) can form 'embryonic germ' (EG) cell colonies (Matsui et al., 1992; Resnick et al., 1992; Durcova-Hills et al., 2006; Durcova-Hills and Surani, 2008; Matsui and Tokitake, 2009). EG cells closely resemble pluripotent embryonic stem (ES) cells derived from the inner cell mass of blastocysts. Furthermore, the fetal origins of testicular cancer hypothesis postulates that XY germ cells that are not controlled appropriately during fetal life can transform into carcinoma in situ (CIS), the pluripotent precursor cells for testicular germ cell tumor (TGCT) (Skakkebæk et al., 1987; Looijenga and Oosterhuis, 1999). In both of these situations, molecular control mechanisms normally involved in suppression of male germ cell pluripotency during fetal life appear to be dysregulated.

Nodal, a member of the TGFβ morphogen family, is a key regulator of early embryonic development known to establish the anterior-posterior axis, specify mesoderm and endoderm during gastrulation, pattern the nervous system and determine left-right asymmetry (Shen, 2007). Nodal signals by binding to activin receptors in the presence of the obligate co-receptor, Cripto (also known as TDGF-1), leading to phosphorylation (activation) of Smad2/3, which regulates transcription of target genes. Lefty1 and Lefty2, also TGFβ molecules, repress the pathway in a dose-dependent manner to limit the range of Nodal signaling. Nodal upregulates its own expression, as well as that of Lefty1 and Lefty2 (Schier, 2003).

The Activin/Nodal class of TGFβs has been linked to the pluripotency of human and rabbit ES cells and pig, mouse and rat epiblast stem cells (EpiSC) in vitro (James et al., 2005; Vallier et al., 2005; Brons et al., 2007; Tesar et al., 2007; Honda et al., 2009; Alberio et al., 2010). In vivo, loss of *Nodal* leads to loss of *Oct4* expression in the epiblast, as well as premature differentiation of epiblast and trophoblast cells (Brennan et al., 2001; Guzman-Ayala et al., 2004; Camus et al., 2006; Mesnard et al., 2006). These

[1]Institute for Molecular Bioscience, The University of Queensland, Brisbane, QLD 4072, Australia. [2]Department of Pathology, Josephine Nefkens Institute, Erasmus MC-University Medical Center Rotterdam, 3015 GE Rotterdam, The Netherlands.

*Author for correspondence (p.koopman@imb.uq.edu.au)

Accepted 3 August 2012

observations prompted us to investigate whether Nodal signaling might play a later role in regulating pluripotency in a differentiated cell lineage, the germ cells, during the organogenesis phase of fetal development.

In this study, we show that Nodal signaling is active in XY but not XX germ cells during mouse gonadal development. Genetic suppression of Nodal signaling led to depressed pluripotency marker expression and early XY germ cell differentiation. Levels of *Cripto* expression and Nodal signaling correlated with propensity of germ cells to de-differentiate and form EG cell colonies in vitro. Finally, although neither *NODAL* nor *CRIPTO* are normally expressed in adult human testes, we found aberrant expression in both patient biopsies positive for CIS and the most malignant TGCT subtypes. Our data indicate a previously unknown role for this pathway in male germ cell development and link dysregulation of this pathway with testis cancer.

MATERIALS AND METHODS

Mice

Protocols and use of animals in these experiments were approved by the Animal Welfare Unit of the University of Queensland. The conditional *Nodal* floxed allele (*Nodal*$^{fl/fl}$) and the *TNAP*^{cre} line were generated as described (Lowe et al., 2001; Lomelí et al., 2000). Embryos were collected from timed matings of the *Nodal*$^{fl/fl}$, CD1 strain, the *W*^{e}/*W*^{e} mutant strain (Buehr et al., 1993) and the Oct4ΔPE:eGFP (OG2) strain (Szabó et al., 2002), with noon of the day on which the mating plug was observed designated 0.5 dpc.

Quantitative RT-PCR

Total RNA was extracted and cDNA generated from gonadal tissue, cultured germ cells or isolated cell pools as described previously (Bowles et al., 2010). Endogenous control primers used to normalize gene expression levels were *Tbp*, *Hprt*, *Sdha*, *Oct3/4* or *Ddx4* (also known as *Myh*) for Taqman analyses, and *Rn18s* or *Tbp* for SYBR analyses; details listed in supplementary material Table S1. Relative transcript abundance was calculated using the $2^{-\Delta CT}$ method. Error bars represent s.e.m. calculated from the independent biological replicates and statistical significance assessed using unpaired (two-tailed) Student's *t*-test.

Germ cell isolation and culture

For pure germ cell isolation, gonadal tissue was collected from Oct4ΔPE:eGFP matings at 10.5 and 11.5 (unsexed) and 12.5, 13.5 and 14.5 dpc (sexed). Tissue was dissociated and germ cell (GFP+) and somatic cell (GFP–) populations were isolated by fluorescence activated cell sorting (FACS) using a FACSAria Cell Sorter (BD Biosciences). For isolation of sub-populations expressing α6-integrin, gonadal tissue was collected from CD1 embryos at 12.5 dpc as described previously (Matsui and Tokitake, 2009) with minor modifications. After dissociation, cells were incubated with FITC-conjugated anti-α6-integrin (CD49F; BD Biosciences, 555735) and/or PE-conjugated anti-SSEA-1 (stage-specific embryonic antigen-1; Bio-Scientific, FAB2155P). Germ cells (anti-SSEA-1+) that were positive and negative for anti-α6-integrin were isolated by FACS using an Influx Cell Sorter (BD Biosciences) and processed for RNA extraction. For analysis of germ cell subpopulations expressing α6-integrin in 12.5 dpc Nodal mutant gonads, single gonad pairs were processed as described above and analyzed using a LSRII Analyzer (BD Biosciences). Statistical significance was determined using a one-way ANOVA. Magnetic isolation of germ cells was performed as described previously (Bowles et al., 2010).

Culture of germ cells and urogenital ridges was performed as described previously (Bowles et al., 2010). Briefly, UGRs were cultured on filters (Millipore, TMTP01300, 5 μm) and germ cells were cultured sparsely (~2000 cells per well) in feeder-free 12-well dishes. Additives to culture were FGF9 (Sigma-Aldrich, 25 ng/ml), basic FGF (FGF2, #1104616, Roche; 25 ng/ml), Nodal (recombinant Mouse, R&D Systems, 100 ng/ml) and FGFR antagonist (SU5402, Calbiochem, 5 mM). Control cultures included dilution vehicle.

Histological and immunofluorescence analysis

In vivo labeling with BrdU labeling reagent (Invitrogen, Cat# 00-0103) was performed by injecting pregnant females intraperitoneally with 1.0 ml/100 g body weight of 1× BrdU. Embryos were harvested 2 hours after BrdU injection, fixed in 4% paraformaldehyde in PBS overnight, dehydrated and paraffin embedded. Immunofluorescence of deparaffinized sections (7 μm) was performed as described previously (Bowles et al., 2010). Primary antibodies used were: anti-DDX4 (AB13840, Abcam; 1:1000), anti-E-Cadherin (#610182, BD; 1:200), anti-Cripto (AB19917, Abcam;1:100), anti-phospho-SMAD2 (#3101, Cell Signaling; 1:300), anti-SMAD2 (AB63576, Abcam; 1:100) and anti-BrdU (#555627, BD; 1:100). Secondary antibodies (all from Molecular Probes; 1:200) were: goat anti-rabbit Alexa Fluor 488, goat anti-rat Alexa Fluor 555 and goat anti-mouse Alexa Fluor 594, and DAPI (D8417, Sigma-Aldrich; 1:2000). Sections were examined by confocal microscopy using a Zeiss LSM-510 META confocal microscope. The number of cells DDX4^{+}/BrdU^{+} and DDX4^{+}/BrdU^{-} (Fig. 3F) and DDX4^{+} cells (supplementary material Fig. S3D) were counted manually in a minimum of 10 sections per gonad of each genotype (*Nodal*$^{+/+}$ and *Nodal*$^{fl/fl}$; *n*=4 and 4). Pair-wise comparisons were analyzed using two-tailed Student's *t*-test.

Western blotting

Western blot was performed by standard protocol on whole gonad-only tissue. Two whole gonads (each Nodal genotype; Fig. 3) or four whole gonads (wild-type analysis; Fig. 1 and supplementary material Fig. S1) were used. Antibodies used were: anti-phospho-SMAD2 (#3101, Cell Signaling, 1:1000), anti-TUBA1A (B-5-1-2, Sigma; 1:1000), anti-DDX4 (AB13840, Abcam; 1:1000), anti-NODAL (AB39242, Abcam; 1:200), goat anti-mouse conjugated to horseradish peroxidase (HRP) (Sigma; 1:2000) and goat anti-rabbit conjugated to HRP (Vector Laboratories; 1:2000). Intensity of PSMAD2 bands was normalized against DDX4 and TUBA1A (Fig. 3C) using Image Lab software (Bio-Rad Laboratories; Version 4.0.1).

Derivation of EG cell colonies

EG derivation was performed as described (Durcova-Hills and Surani, 2008) with minor modifications. Briefly, 12.5 dpc Nodal$^{+/+}$, Nodal$^{fl/+}$ or Nodal$^{fl/fl}$ single gonad-only pairs were dissociated and seeded onto one well of a six-well culture plate (NUNC) containing 4×10^{5} cells/ml of Mitomycin C-treated STO cells. Cells were incubated in PGC growth media (Durcova-Hills and Surani, 2008), changed daily for 10 days. Wells were stained for AP activity using the AP staining kit (Sigma, 86-R) as per manufacturer's instructions. The total number of AP-positive, densely packed colonies was counted for each well. Statistical significance was assessed by one-way ANOVA followed by a post-test for linear trend.

Analysis of human germ cell tumors

Use of the patient tissues is approved by an institutional review board (MEC 02.981). Samples were used according to the 'Code for Proper Secondary Use of Human Tissue in The Netherlands', from the Dutch Federation of Medical Scientific Societies (FMWV, version 2002). Tissues were collected as described (Looijenga et al., 2003), and tumors were diagnosed according to WHO standards by an experienced pathologist (J. Wolter Oosterhuis, Erasmus MC, Rotterdam, The Netherlands). The testicular parenchyma samples investigated have been described previously (Mosselman et al., 1996). qRT-PCR was performed on a 7900HT Fast Real-Time PCR System (Applied Biosystems).

RESULTS

Nodal signaling is active in fetal XY germ cells

We have previously conducted a genome-wide microarray analysis of gene expression in mouse fetal gonads (Holt et al., 2006). Subsequent analysis showed that a number of genes associated with the Nodal signaling pathway were expressed more highly in XY compared with XX gonads at 12.0 dpc. Using quantitative reverse transcriptase-PCR (qRT-PCR), we confirmed that *Nodal*, *Cripto*, *Lefty1* and *Lefty2* are predominantly expressed in XY but

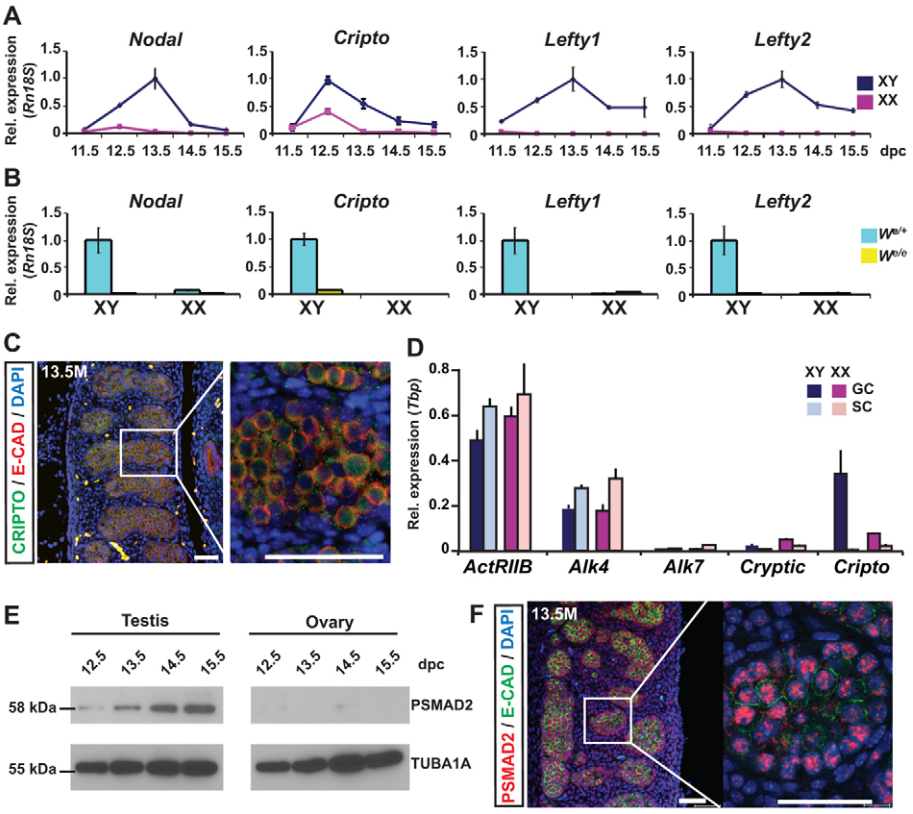

Fig. 1. The Nodal/Cripto signaling pathway is active in mouse XY fetal germ cells. (**A**,**B**) *Nodal*, *Cripto*, *Lefty1* and *Lefty2* are expressed predominantly in XY gonads at 12.5-15.5 dpc (A) and their reduced expression in W^e/W^e germ cell-less gonads (B) indicates expression by germ cells (n=3). Highest level of gene expression was set as 1. (**C**) Nodal receptor Cripto (green) is detected on the surface of 13.5 dpc XY germ cells marked with E-cadherin (red); DAPI marks nuclei (blue). (**D**) The activin receptors *Acvr2b* and *Alk4,* but not *Alk7*, are detectable in XX and XY germ cells (GC) and gonadal somatic cells (SC) at 13.5 dpc. Expression of *Cripto* is expressed by XY germ cells, but the alternative receptor *Cryptic* is not expressed a substantial level (n=3). (**E**) Phospho-Smad2 was detected by western blot within wild-type XY gonad-only samples at 12.5-15.5 dpc but was absent from XX samples. Tuba1a was used as the loading control. (**F**) Phospho-Smad2 (PSMAD2; red) was detected strongly in the nucleus of 13.5 dpc XY germ cells marked with E-cadherin (green). Nuclei are counterstained with DAPI (blue). Expression was normalized to *Rn18s* (A,B) and *Tbp* (D). Scale bars: 100 μm.

not XX mouse fetal gonads at 12.5-15.5 dpc (Fig. 1A); in all cases, expression was negligible at 11.5 dpc, peaked at 12.5 (*Cripto*) or 13.5 dpc (*Nodal*, *Lefty1*, *Lefty2*), and had mostly subsided by 14.5 dpc. We also investigated expression of *Nodal* and *Cripto* in purified germ cell populations at 11.5-14.5 dpc (to account more accurately for germ cell numbers) and detected peak expression at 13.5 and 12.5 dpc, respectively (supplementary material Fig. S1A,B). Lack of expression of all four Nodal pathway genes in W^e mutant gonads, which are devoid of germ cells, suggested that these genes are either expressed by the germ cells of the fetal testis or depend on the presence of germ cells (Fig. 1B). Expression of all four genes began at least a day earlier than that of *Nanos2*, which was previously the earliest known male-specific germ cell marker and encodes a protein essential for male germ cell fate commitment (Tsuda et al., 2003; Suzuki and Saga, 2008).

The obligate Nodal co-receptor Cripto was localized to the surface of XY germ cells at 13.5 dpc, consistent with a role in regulating Nodal signaling in the germline (Fig. 1C). Interstitial and other somatic cells of the testis were negative for Cripto expression. In addition to Cripto, the activin receptors ActRIIB (Acvr2b – Mouse Genome Informatics), Alk4 or Alk7 are also required for Nodal signaling (Shen, 2007). *Acvr2b* and *Alk4* were detected in both purified germ and somatic cells in XY and XX gonads at 13.5 dpc (Fig. 1D). Expression of *Alk7* or the alternative Nodal co-receptor *Cryptic* were not detected at appreciable levels at this time (Fig. 1D). Quantitative RT-PCR analysis on purified germ cell and somatic cell populations (supplementary material Fig. S1B) confirmed male-specific *Cripto* expression restricted to germ cells. Although some activin receptors are broadly expressed, the highly cell-specific *Cripto* and *Nodal* expression (Fig. 1B-D; supplementary material Fig. S1B) suggests that Nodal action is limited to germ cells within the gonad.

Using western blot analysis, we could detect Nodal protein in whole XY gonads from 13.5-15.5 dpc (supplementary material Fig. S1C). To investigate whether Nodal signaling is actively engaged in male germ cells, we tested for the presence of phospho-Smad2 (P-Smad2), an indicator of active activin/Nodal signaling. By western blot, P-Smad2 was detected within fetal testes but not ovaries at 12.5-15.5 dpc (Fig. 1E). Using immunofluorescence, we found that P-Smad2 was largely restricted to the germ cells of 13.5 dpc testes (Fig. 1F). Given the restricted expression of Cripto, the low level of P-Smad2 detected in somatic cells is likely to reflect non-Nodal TGFβ signaling in these cells (Mendis et al., 2010). Together, these results indicate that activin/Nodal signaling is active in fetal XY germ cells, but not XX germ cells or gonadal somatic cells, in the crucial 12.5-14.5 dpc period when their proliferation is arrested and commitment to spermatogenic differentiation is stimulated.

Cripto expression responds to Fgf9

Recently, we showed that the signaling molecule Fgf9, which is highly expressed in the developing testis at 11.5 dpc, promotes male germ cell fate (Bowles et al., 2010). In addition, XY, but not XX, germ cells become dependent on Fgf9 by about 12.5 dpc (DiNapoli et al., 2006). Given the upregulation of *Cripto* in XY germ cells between 11.5 and 12.5 dpc (Fig. 1A) we reasoned that its expression might be triggered by Fgf9. To test this hypothesis, we carried out urogenital ridge (UGR) organ culture experiments: *Cripto* expression was increased by Fgf9 (Fig. 2A) and decreased in the presence of an FGF receptor antagonist (Fig. 2B). *Nanos2*, a marker of male germ cell fate (Suzuki and Saga, 2008), was used as a control in these experiments. In XY *Fgf9*-knockout mice, expression of both *Nodal* and *Cripto* was low (data not shown), as would be expected, as XY *Fgf9*-null gonads (including resident

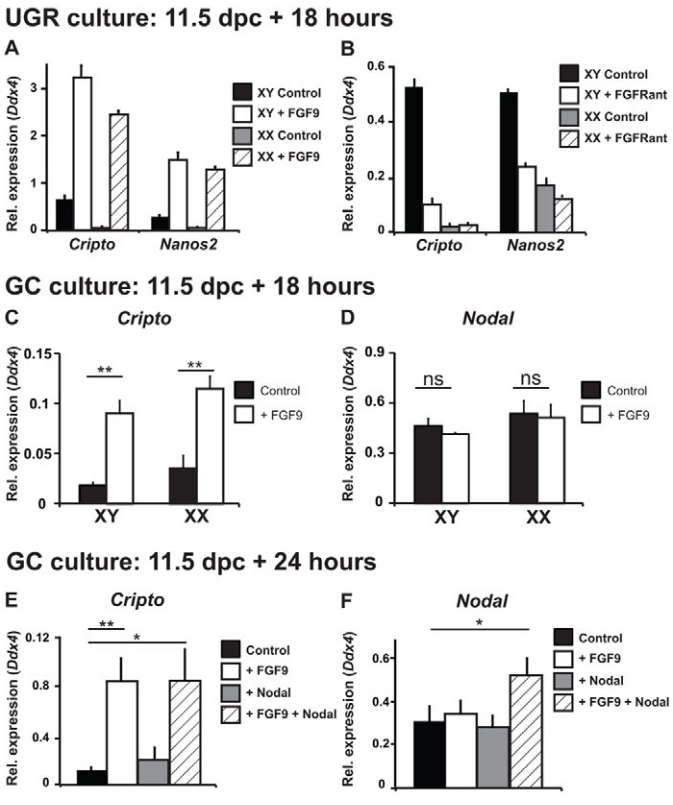

Fig. 2. *Cripto* expression responds to Fgf9 in vitro. (**A**) In 11.5 dpc XX and XY urogenital ridge cultures, Fgf9 induces *Cripto* expression; *Nanos2* is used as a control that responds to Fgf9. (**B**) A FGFR antagonist suppresses *Cripto* expression in 11.5 dpc XY and XX urogenital ridge cultures; *Nanos2* is also suppressed. (**C**) Fgf9 induces *Cripto* expression in XY and XX isolated 11.5 dpc germ cells cultured for 18 hours. (**D**) Fgf9 treatment of isolated XY and XX 11.5 dpc germ cells does not induce *Nodal* expression after 18 hours of culture. (**E**) Fgf9 treatment, but not Nodal treatment, of isolated unsexed 11.5 dpc germ cells induces *Cripto* expression after 24 hours in culture. (**F**) Treatment of 11.5 dpc unsexed germ cells with Fgf9 in addition to exogenous Nodal induces *Nodal* expression after 24 hours. Expression was normalized to *Ddx4* (A-F) and the highest level of gene expression was set as 100 in A and B. Statistical significance was assessed using Student's *t*-test (C,D) and one-way ANOVA with a Dunnett's post-test for multiple comparisons (E,F); error bars represent s.e.m. of four independent experiments, each performed in duplicate (C-F) and s.d. of technical replicates for one representative experiment (A,B); $*P<0.05$, $**P<0.005$. ns, not significant.

germ cells) undergo complete male-to-female sex reversal (DiNapoli et al., 2006; Bowles et al., 2010).

We next confirmed that Fgf9 acts directly on isolated germ cells to induce *Cripto* expression (Fig. 2C). Both XX and XY germ cells behaved similarly under these conditions, suggesting that the presence of Fgf9, rather than the chromosomal constitution of the germ cells, ensures that *Cripto* is specifically induced in male germ cells in vivo.

Although Fgf9 triggered *Cripto* expression, there was no concomitant upregulation of *Nodal* expression in isolated 11.5 dpc germ cells cultured for 18 hours (Fig. 2D). However, in intact UGR cultures, which were started at 11.5 dpc and continued for 18 hours, Fgf9 induced expression of both *Cripto* and *Nodal* (supplementary material Fig. S2). We hypothesized that the differing observations with respect to *Nodal* upregulation reflect the close clustering of germ cells in the UGR system versus the sparse distribution of germ cells in purified germ cell culture. We propose a mechanism whereby FGF9 triggers Cripto expression in germ cells and that this allows Nodal, which is initially present at low levels, to feedback and upregulate its own expression in germ cells. Such a mechanism is consistent with our observation that Cripto expression peaks earlier than Nodal expression (Fig. 1A). In support of this model, we found that when dispersed germ cells were cultured in Fgf9 (to trigger *Cripto* expression) and exogenous Nodal, expression of *Nodal* was induced (Fig. 2E,F).

Suppressed Nodal signaling leads to precocious XY germ cell differentiation

In vitro, activin/Nodal signaling has been implicated in the maintenance of the undifferentiated state in mammalian EpiSC and ES cells (James et al., 2005; Vallier et al., 2005; Brons et al., 2007; Tesar et al., 2007; Honda et al., 2009; Alberio et al., 2010). These findings prompted us to investigate whether Nodal signaling might play an analogous role during male germ cell development. To address this question, we attempted conditional deletion of *Nodal* by crossing $Nodal^{fl/fl}$ mice, in which *Nodal* exons 2 and 3 are flanked by *loxP* recombination sites (Lowe et al., 2001), with the $TNAP^{cre}$ strain of mice that expresses Cre recombinase in germ cells (Lomelí et al., 2000). We were unable to obtain conditional mutant embryos, perhaps owing to ectopic Cre recombinase expression in the $TNAP^{cre}$ strain (Kehler et al., 2004; reviewed by Hammond and Matin, 2009) and/or the reduced expression of Nodal (hypomorphism) in the $Nodal^{fl/fl}$ strain prior to recombination (Lowe et al., 2001). For this reason, we based all further studies on hypomorphic $Nodal^{fl/fl}$ embryos, which displayed ~30% of wild-type testicular *Nodal* expression (Fig. 3A) and survive to adulthood.

Immunofluorescence staining for the germ cell marker DDX4 was indistinguishable between $Nodal^{fl/fl}$ and wild-type gonads at 11.5 dpc (supplementary material Fig. S3A); this timepoint is prior to germ cell expression of *Nodal* at 12.5 dpc (Fig. 1A), but after the requirement for Nodal during gastrulation. The equivalent DDX4 expression indicates that germ cell specification and migration occur normally in $Nodal^{fl/fl}$ mutant embryos. DDX4 expression and germ cell numbers were also comparable between genotypes at later stages (13.5, 14.5 and 17.5 dpc) of gonad development (supplementary material Fig. S3A,B). Together, these data indicate that there is no substantial loss of germ cells due to decreased *Nodal* expression in $Nodal^{fl/fl}$ embryonic gonads. We therefore questioned whether XY germ cells deficient in *Nodal* were qualitatively abnormal.

To determine the effect of greatly reduced Nodal signaling in XY germ cells, we first examined P-Smad2 expression in gonads of the hypomorphic $Nodal^{fl/fl}$ mouse strain. Diminished levels of P-Smad2 (but not SMAD2) in 14.5 dpc XY $Nodal^{fl/fl}$ gonads relative to wild type (Fig. 3B,C; and data not shown) revealed that the majority of Smad2 activation in the gonad was specifically dependent on Nodal signaling, and was not part of a more generalized response to other TGFβ signaling.

We next assayed markers of pluripotency and male germ cell differentiation in $Nodal^{fl/fl}$ gonads. We detected reduced expression of pluripotency markers *Nanog*, *Sox2* and *Oct3/4*, and, conversely, increased expression of male germ cell differentiation markers *Nanos2*, *p15* and *Dnmt3l* in $Nodal^{fl/fl}$ gonads, relative to wild type at 14.5 dpc (Fig. 3D). Because this finding suggested early differentiation of germ cells, we examined the total cohort of germ cells 1 day earlier, when arrest was not yet complete and differences in proliferation might be detected. BrdU incorporation

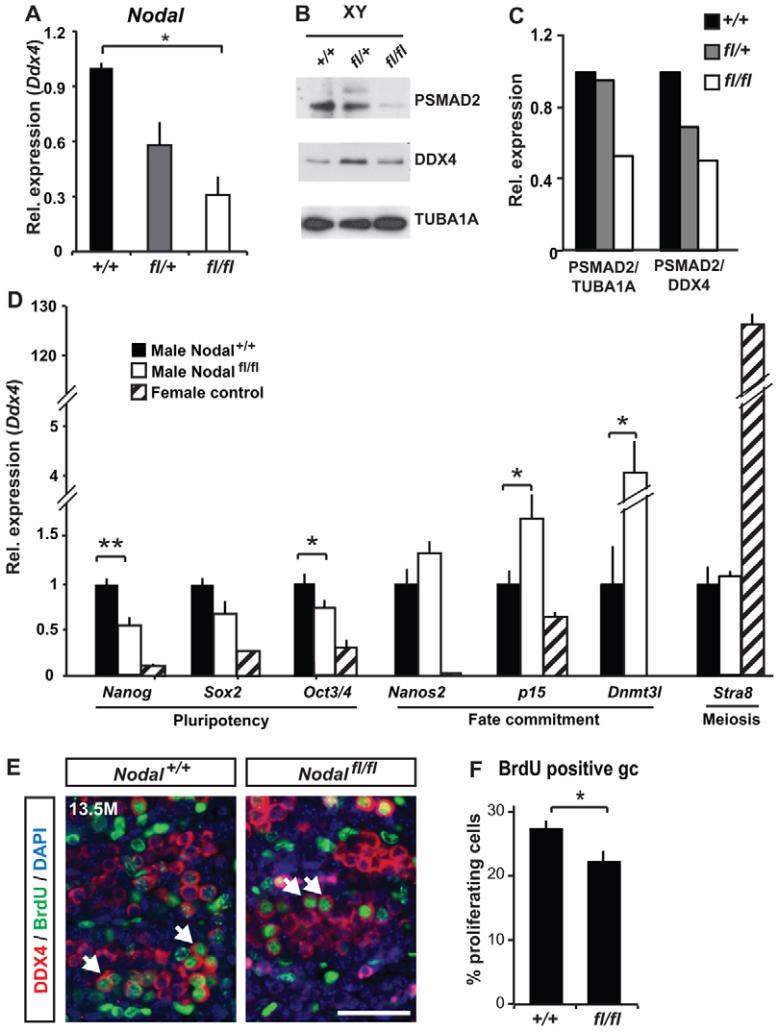

Fig. 3. Compromised Nodal signaling leads to premature differentiation and reduced pluripotency. (**A**,**B**) *Nodal* mRNA (A) and phospho-Smad2 protein (B) expression is reduced in XY *Nodal*$^{fl/fl}$ gonads at 14.5 dpc. Ddx4 and Tuba1a are germ cell and total protein loading controls, respectively; *n*=3, 3 and 3 (A) and *n*=2, 2 and 2 (B). (**C**) Relative P-Smad2 expression from (B) normalized against Tuba1a and Ddx4. (**D**) Pluripotency markers (*Nanog*, *Sox2* and *Oct3/4*) are decreased and male differentiation markers (*Nanos2*, *p15* and *Dnmt3l*) are increased in 14.5 dpc male *Nodal*$^{fl/fl}$ gonads; meiosis marker *Stra8* was unchanged between samples; female gonads were used as a control, *n*=3 and 3. (**E**) BrdU incorporation (green) was assessed in germ cells (red; Ddx4) of 13.5 dpc *Nodal*$^{+/+}$ and *Nodal*$^{fl/fl}$ XY gonads, and was decreased in *Nodal*$^{fl/fl}$ germ cells compared with wild-type controls. Scale bars: 100 μm. (**F**) 27.8% of wild-type germ cells were proliferating (BrdU positive) at 13.5 dpc, in contrast to only 22.3% in *Nodal*$^{fl/fl}$ gonads; *n*=4 and 4. Expression was normalized to *Ddx4* (A,D) and wild-type gene expression was set as 1. Error bars represent s.e.m. of three independent experiments, each performed in triplicate; statistical significance was assessed using Student's *t*-test; **P*<0.05, ***P*<0.005. Scale bars: 100 μm.

revealed that 27.8% of wild-type germ cells were proliferating at 13.5 dpc, in contrast to only 22.3% of *Nodal*$^{fl/fl}$ germ cells (Fig. 3E,F). This 5% difference in proliferating germ cell number, though significant, was not manifest in total germ cell numbers at 13.5, 14.5 and 17.5 dpc (supplementary material Fig. S3B), possibly owing to the sensitivity of our counting methods.

Last, because Fgf9 induces Nodal signaling via *Cripto* expression (Fig. 2), and because it is also important for suppression of XY germ cell meiosis (Bowles et al., 2010), we investigated the meiosis marker *Stra8* in our in vivo model of suppressed Nodal signaling. However, in *Nodal*$^{fl/fl}$ mutant gonads, *Stra8* expression was not induced in XY germ cells at 14.5 dpc (Fig. 3D). Together, our data suggest that when Nodal signaling is diminished, fetal XY germ cells express markers of male fate commitment and cease proliferation earlier than normal.

High Cripto expression characterizes a highly pluripotent sub-population of germ cells

Previous studies have shown that mouse fetal germ cells are heterogeneous with respect to cell-surface properties and ability to generate pluripotent EG colonies in vitro. Matsui and Tokitake (Matsui and Tokitake, 2009) flow-sorted mouse fetal germ cells based on α6-integrin expression, and identified an α6-integrin-low population of germ cells with 2.5-fold higher proclivity for forming EG colonies. Because our in vivo findings linked Nodal signaling with maintenance of pluripotency marker expression in germ cells, we investigated whether expression of Nodal signaling components characterized this sub-population of germ cells with the greatest potential to undergo reprogramming to stem cells.

We flow-sorted 12.5 dpc germ cells (SSEA-1-positive) into α6-integrin-negative and -positive pools (Fig. 4A; supplementary material Fig. S4A,B), and assessed expression of *Cripto*, *Nodal*, *Lefty1*, *Lefty2* and the pluripotency markers *Sox2*, *Oct3*/*4* and *Nanog* in each by qRT-PCR. The α6-integrin-negative population displayed higher expression of all markers than the α6-integrin-positive population, with *Cripto*, *Nodal* and *Lefty2* exhibiting the greatest difference (2.08, 1.93 and 2.04 fold, respectively) of all genes tested (Fig. 4B). These data indicate that, although Nodal signaling genes appear to be expressed by all XY fetal germ cells (Fig. 1C), highest expression of these characterizes the same subpopulation of fetal testicular germ cells previously identified as particularly pluripotent (Matsui and Tokitake, 2009).

Suppressed Nodal signaling reduces the efficiency of EG cell derivation

We next investigated the effects of reduced Nodal signaling on EG colony derivation. We cultured 12.5 dpc explanted testes from wild-type, *Nodal*$^{+/fl}$ and *Nodal*$^{fl/fl}$ embryos under EG colony-forming conditions; at this timepoint in *Nodal*$^{fl/fl}$ gonads, *Nodal* and *Cripto* expression levels are ~20% and ~70% of wild-type levels

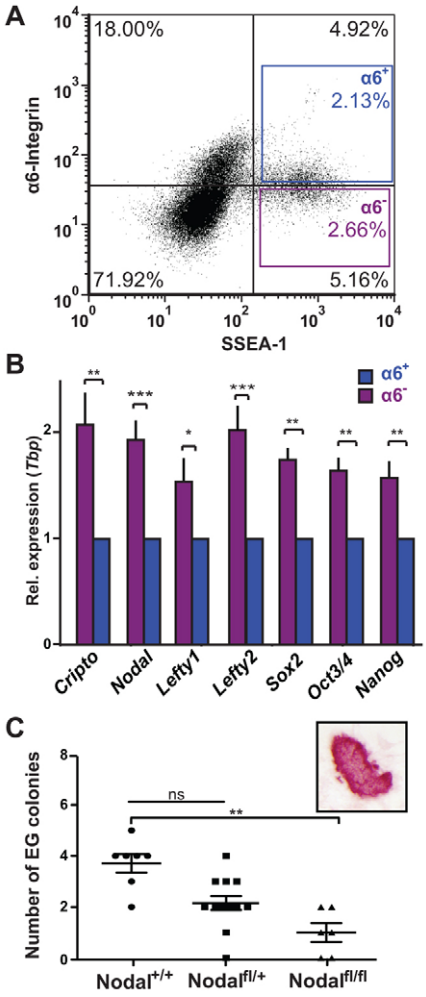

Fig. 4. Nodal signaling determines germ cell pluripotency. (**A**) FACS analysis of 12.5 dpc germ cells (Ssea1 positive), separated into α6-integrin-negative (2.66%; $\alpha6^-$) and -positive (2.13%; $\alpha6^+$) populations. (**B**) Expression of *Cripto*, *Nodal*, *Lefty1*, *Lefty2*, *Sox2*, *Oct3/4* and *Nanog* in populations from A is higher in α6-integrin-negative germ cells, n=5. Expression was normalized to *Tbp* and gene expression of the α6-integrin-positive population was set to 1. Statistical significance was assessed using Student's t-test; error bars represent s.e.m.; *P<0.05, **P<0.005, ***P<0.0005; ns, not significant. (**C**) EG colonies were derived at a significantly lower rate from $Nodal^{fl/fl}$ than $Nodal^{+/+}$ 12.5 dpc XY gonad pairs, based on alkaline phosphatase staining (inset) after 10 days of culture; n=7, 15 and 6. Statistical significance was assessed using one-way ANOVA; bars represent mean±s.e.m.; **P<0.005; ns, not significant.

respectively. Total germ cell numbers, indicated by *Ddx4* expression, remained comparable with wild-type gonads (supplementary material Fig. S4C), as did the ratio of α6-integrin-negative to α6-integrin-positive germ cells assessed by flow cytometry (supplementary material Fig. S4D). In the EG colony derivation assay, each wild-type gonad pair generated 3.7±0.35 alkaline phosphatase-positive EG cell colonies (n=7), whereas 1.0±0.33 EG cell colony arose from each $Nodal^{fl/fl}$ gonad pair (n=6; Fig. 4C). Thus, reduced Nodal signaling leads to reduced stem cell potential of the total XY fetal germ cell population.

EG cell derivation requires the application of three factors: FGF2, LIF and SCF (Matsui et al., 1992; Resnick et al., 1992; Durcova-Hills et al., 2006; Durcova-Hills and Surani, 2008). We found that FGF2, like FGF9, can induce *Cripto* expression in 10.5 and 12.5 dpc XX and XY germ cells (supplementary material Fig. S4E), suggesting that its role during in vitro transformation of germ cells to EG colonies may be to stimulate *Cripto* expression, thereby enhancing pluripotency in those cells.

Nodal signaling components are overexpressed in human testis cancers

CRIPTO was first identified from a human embryonal carcinoma cell line, NTERA2 (Ciccodicola et al., 1989), and a later study indicated that CRIPTO is expressed in some non-seminoma germ cell tumors (Baldassarre et al., 1997). Most recently, heterogeneous expression of CRIPTO within the human teratoma-derived NTERA2 cell line identified $CRIPTO^{High}$-expressing cells as those having the greatest tumorigenic potential and most undifferentiated phenotype (Watanabe et al., 2010). Our data identifying a function for Cripto during normal XY fetal germ cell development led us to speculate that CRIPTO expression may be maintained or re-activated in carcinoma in situ (CIS), a tumor stem cell thought to arise from fetal germ cells that fail to fully differentiate and are retained in a dormant, pluripotent state in the adult testis (Skakkebæk et al., 1987; Looijenga et al., 2003; de Jong et al., 2008; Gillis et al., 2011). Currently, no CIS model exists in mice (Oosterhuis and Looijenga, 2005; Looijenga et al., 2011), precluding a test of this hypothesis in an experimental model system. For this reason, we examined *NODAL*, *CRIPTO* and *LEFTY* expression by qRT-PCR in a range of human testis biopsies containing CIS cells. In support of our hypothesis, we found highest expression of *CRIPTO*, *NODAL* and *LEFTY1* in those biopsies in which over 90% of tubules contained CIS (Fig. 5A-C). The low levels of normalized gene expression reflect the fact that CIS cells in these biopsies make up a very small proportion of total cells.

All CIS ultimately progresses to either seminoma, a tumor type composed of cells expressing fetal germ cell markers, or non-seminoma, a diverse class of tumors including embryonal carcinoma (EC), yolk sac tumor (YST), teratoma and choriocarcinoma, that express a range of pluripotency markers (Skakkebæk et al., 1987; Looijenga, 2009). Therefore, we next tested whether Nodal pathway genes are upregulated in these various testis cancers. We detected strong expression of *CRIPTO* and *NODAL* in the invasive tumor types EC and YST, and varied expression in mixed non-seminomas (mNS; Fig. 5D,E). Little or no expression was associated with the benign tumors teratoma and choriocarcinoma. *LEFTY1* was overexpressed only in YST and mNS (Fig. 5F); the absence of the NODAL inhibitor LEFTY1 in EC may underlie its highly malignant phenotype (Postovit et al., 2008). Within the mNS samples, which contain some differentiated and some non-differentiated tissue, levels of *CRIPTO*, *NODAL* and *LEFTY1* expression were in direct proportion to the pluripotent EC and YST cell content of each tumor (Fig. 5G-I). None of these genes was overexpressed in seminomas or other types of germ cell tumor (supplementary material Fig. S5A-C); the lack of *NODAL/CRIPTO* expression may indicate that CIS cells reduce their malignant behavior as they progress to seminoma. Together, these results suggest that the Nodal pathway is activated in TGCTs and is specifically associated with germ cell tumor pluripotency and invasiveness, rather than being a cancer marker per se.

DISCUSSION

The Nodal signaling pathway is known to play important roles in pattern formation during embryogenesis in a number of vertebrate

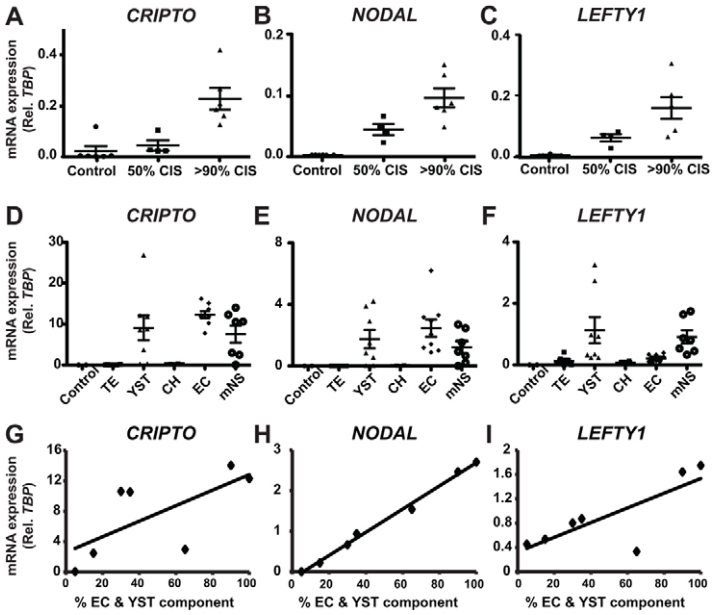

Fig. 5. *CRIPTO*, *NODAL* and *LEFTY1* are overexpressed in human malignant testicular germ cell tumors. (**A-C**) Expression of *CRIPTO*, *NODAL* and *LEFTY1* increases with increasing percentage of CIS-containing tubules in human adult testis samples; *n*=6, 4 and 6. (**D-F**) *CRIPTO* and *NODAL* expression is upregulated in the pluripotent tumors embryonal carcinoma (EC), mixed non-seminoma (mNS) and yolk sac tumor (YST). *LEFTY1* expression is increased in YST and mNS but not EC, teratoma (TE) or choriocarcinoma (CH); *n*=6, 8, 2, 9 and 7. (**G-I**) Expression of *CRIPTO, NODAL* and *LEFTY1* increases in mNS tumors in proportion to pluripotent EC and YST cell content. Linear regression lines are shown, and coefficient of determination (R^2) values are: 0.461 (*CRIPTO*), 0.994 (*NODAL*) and 0.619 (*LEFTY1*). Expression normalized to *TBP*; data represent mean±s.e.m.

species. The present study expands the known developmental roles of Nodal signaling by demonstrating that this pathway is transiently active in male mouse fetal germ cells just prior to and during the period of their sexual fate determination. We find that the germ cells with the highest propensity to form pluripotent EG cell lines in vitro are those that express the highest levels of Nodal signaling genes. Hence, our studies suggest that the role of Nodal during germ cell development is to regulate the timing of the transition from proliferation to differentiation in the male germline during fetal life. Finally, the observation that Nodal signaling is reactivated ectopically in adult human TGCT provides a potential link between fetal germ cell regulation and adult disease.

Investigating the regulation of Nodal signaling, we found that Fgf9, which is expressed by the somatic cells of the testis, triggers male germ cells to upregulate *Cripto* expression around 12.0-12.5 dpc, shortly after germ cell colonization of the developing testis (supplementary material Fig. S6). This upregulation enables Nodal, presumably present at low endogenous levels, to upregulate its own expression and that of downstream targets *Lefty1* and *Lefty2*, peaking at 13.5 dpc. We have previously shown that Fgf9 acts to make XY germ cells more resistant to entering meiosis, through an unknown mechanism (Bowles et al., 2010). Hence, an obvious hypothesis was that FGF9 acts on XY germ cells to trigger Nodal signaling and thereby make those cells less likely to enter meiosis. However, this hypothesis is not supported by our data: knockdown of Nodal to 30% of normal levels had no effect on expression of pre-meiotic gene *Stra8* (Fig. 3D), although complete deletion of *Nodal* is required to confirm this. Instead, our data suggest that the role of Nodal signaling in XY germ cells is to extend the period of pluripotency and delay the onset of differentiation. Following this transient expression of Nodal pathway genes, TGFβ and activin signaling evidently act to ensure correct G1/G0 arrest (Mendis et al., 2010; Moreno et al., 2010). The expression of Cripto by XY germ cells may make such cells temporarily resistant to the effect of TGFβ and activin ligands, as has been suggested in other systems (Gray et al., 2003; Gray et al., 2006). Diminished expression of *Cripto* at these later time points, presumably owing to a decrease in FGF9 signaling, should allow testicular germ cells to become gradually responsive to other TGFβ factors. An interesting possibility raised by our study is that FGF signaling might play a similar role in other situations where Nodal signaling has been implicated.

Our data indicate a role for Nodal signaling in regulating germ cell potency in vivo. First, fetal germ cells from a genetic model of reduced Nodal signaling are compromised in their ability to generate pluripotent EG cell lines in culture. Second, the gonadal germ cell fraction most competent to form EG cell lines in vitro (Matsui and Tokitake, 2009) is that which expresses the highest levels of Nodal signaling genes. These observations are consistent with several in vitro studies linking TGFβ/activin/Nodal signaling to cell pluripotency. James et al. (James et al., 2005) showed that Smad2/3 is active in undifferentiated human ES cells, and that chemical inhibition of activin receptor Alk4/5/7, using SB431542, suppresses expression of the pluripotency marker *Oct4* in mouse blastocyst outgrowths during ES cell derivation in culture. Similarly, SB431542 was found to reduce Smad2/3 phosphorylation and Oct4 expression in cultured rabbit ES cells (Honda et al., 2009), and to promote differentiation/suppress pluripotency markers in pig (Alberio et al., 2010) and mouse (Tesar et al., 2007) epiblast stem cells. However, it is important to note that these effects cannot be attributed specifically to Nodal signaling, as SB431542 blocks signaling mediated by the entire TGFβ/Activin/Nodal branch of the TGFβ superfamily.

One factor that is crucial for in vitro derivation of EG colonies from fetal germ cells is FGF2. We found that FGF2, like FGF9, was able to induce *Cripto* expression in fetal gonadal germ cells. We propose that a role (if not the role) of FGF2 during in vitro transformation of germ cells to EG colonies is to upregulate or induce *Cripto* expression, thereby triggering Nodal signaling and enhancing pluripotency potential in those cells (Fig. 6). Interestingly, unlike LIF and SCF, FGF2 is required only for the first 24 hours of EG derivation (Durcova-Hills et al., 2006); a merely transient requirement for FGF2 could be explained if its role is simply to trigger the upregulation of *Cripto* that facilitates amplification of Nodal signaling.

It has recently been reported that Nodal expression in XY germ cells functions to make them resistant to meiotic induction (Souquet et al., 2012). By adding a chemical inhibitor (SB431542)

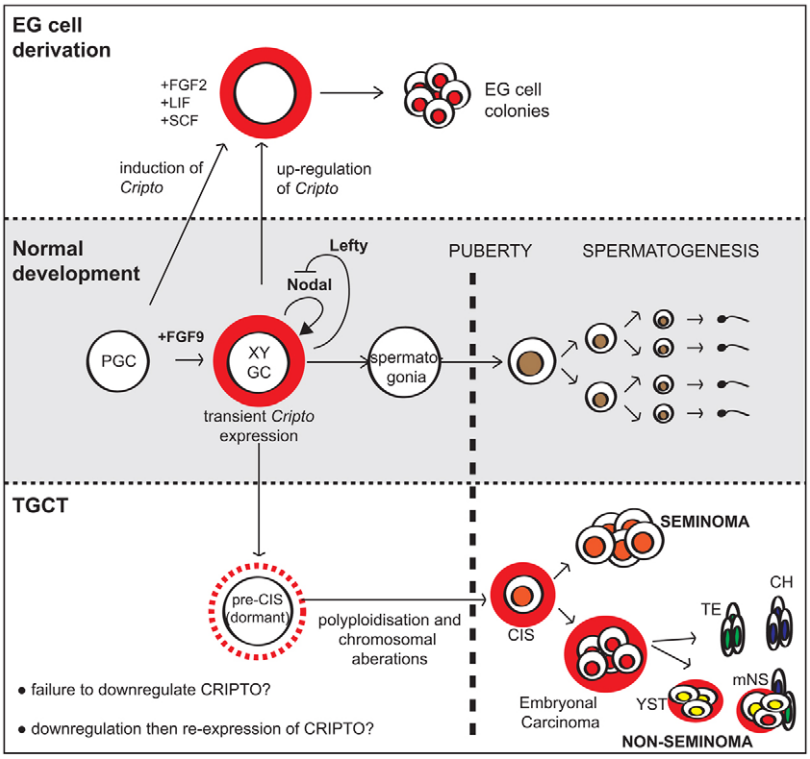

Fig. 6. Model of Cripto expression during normal germ cell development, EG colony derivation and TGCT. During normal germ cell development, Cripto is transiently expressed (red halo), coinciding with active Nodal signaling, to maintain pluripotency. Under EG-forming conditions, *Cripto* expression is induced in 10.5 dpc germ cells (normally *Cripto* negative) and is increased above normal levels in 12.5 dpc germ cells (normally *Cripto* positive). Under pathological conditions (in the human), gonocytes that fail to undergo correct spermatogenic differentiation but retain expression of pluripotency markers develop into dormant, pre-carcinoma in situ (pre-CIS) cells during infancy. Following puberty, pre-CIS cells accumulate genomic aberrations to become CIS cells, the precursor cell for seminoma and non-seminoma germ cell tumors that are positive for *CRIPTO* expression. Whether expression of *CRIPTO* is retained or reactived during malignant transformation is unknown. *CRIPTO* expression is lost during CIS progression into seminoma. Conversely, *CRIPTO* expression is retained during CIS progression into embryonal carcinoma, yolk sac tumor (YST) and mixed non-seminoma (mNS) tumors with high percentages of embryonial carcinoma and YST. Teratoma (TE) and choriocarcinoma (CH) are negative for CRIPTO expression.

of activin receptors Alk4, Alk5 and Alk7 to cultured mouse fetal testes explanted at 11.5 dpc, Souquet et al. (Souquet et al., 2012) found that some XY germ cells enter meiosis. Conversely, when exogenous Nodal was added to cultured female gonads, a reduction in the number of meiotic germ cells was observed. In our in vivo model of suppressed Nodal signaling, *Stra8* expression was not induced in XY germ cells of $Nodal^{fl/fl}$ gonads at 14.5 dpc (Fig. 3D), as might be expected if the role of Nodal was to suppress meiosis. However, because Nodal expression is reduced, not ablated, in our model, a role in suppressing meiosis can not be excluded. Differences between endogenous and exogenous systems may account for the different conclusions, therefore analysis of a complete conditional null mutant will be required to determine whether Nodal suppresses meiosis in vivo. A further discrepancy between the two studies relates to the temporal profile of Nodal signaling gene expression. Souquet et al. (Souquet et al., 2012) reported that expression of *Nodal*, *Cripto*, *Lefty1* and *Lefty2* is highest at 11.5 dpc and declines thereafter. Our experiments indicated peak expression at 12.5 (*Cripto*) and 13.5 dpc (*Nodal*, *Lefty1* and *Lefty2*; Fig. 1A), consistent with human *Nodal* expression and phospho-SMAD2 activation predominant from 13.5 dpc onwards. The disparity between our gene expression studies can most likely be attributed to differences in normalizer genes used. When normalizing against *Ddx4* expression we observed the same expression profile reported by Souquet et al. (Souquet et al., 2012) (data not shown); however, because expression of *Ddx4* increases in germ cells over time, it is considered an unsuitable normalizer for dynamic studies of germ cell gene expression (van den Bergen et al., 2009). Using a more appropriate normalizer, *Oct3/4*, which is stable in XY germ cells over this timecourse (van den Bergen et al., 2009), we observed peak expression in purified germ cells at 12.5 and 13.5 dpc for *Cripto* and *Nodal*, respectively (supplementary material Fig. S1B), as we also found when analyzing gene expression in whole gonads (Fig. 1A).

Finally, we found a strong correlation between Nodal pathway gene expression and malignant TGCTs. In previous studies, expression of CRIPTO has been observed in a variety of carcinomas, including mammary, pancreas, intestine and skin cancer (Strizzi et al., 2005). In these situations, CRIPTO has emerged as an oncogenic growth factor, controlling proliferation, migration and survival (Bianco et al., 2005; Wechselberger et al., 2005), but it remains unclear whether this involvement reflects the role of Cripto in Wnt signaling, Src activation through glypican binding or Nodal signaling (Bianco et al., 2010). Our data strongly correlate CRIPTO expression with TGCT, and specifically implicate dysregulation of the Nodal pathway in carcinogenesis, at least in the context of TGCT.

TGCT is an unusual cancer in that it appears to be seeded during fetal life, yet only manifests after puberty and during young adulthood (Skakkebæk et al., 1987; Looijenga et al., 2011). It is widely believed, based largely on chromatin modification studies, that XY germ cells that do not undergo correct differentiation during fetal development are able to survive as dormant pre-CIS cells in the testis until, at puberty, they are reactivated to form CIS cells that then progress to either seminoma or non-seminoma. Our studies indicate that *CRIPTO*/*NODAL* expression is activated ectopically in CIS cells and in the most pernicious forms of TGCT in humans (Fig. 6). It is not yet clear whether *CRIPTO* expression fails to be downregulated in some germ cells during fetal life, or whether *CRIPTO* expression is re-initiated in some germ cells during adult life. Our results strongly support a model whereby TGCT is triggered by ectopic action of a program that normally operates only during fetal germ cell development.

Our results have important implications for the etiology and management of testicular cancer. Mechanistic studies of testis cancer biology have been hampered by the lack of a mouse model of CIS, and our results raise the possibility that sustained expression of *Cripto* in transgenic mouse germ cells may provide

such a model. Second, being a cell-surface protein, CRIPTO may prove a tractable target for testicular cancer treatment, as it has proven for various CRIPTO-positive solid tumors (Kelly et al., 2011). Finally, detection of cleaved CRIPTO in human semen may offer a non-invasive method of clinical diagnosis of a variety of testis cancers, a possibility now under investigation.

Acknowledgements
We thank M. Kuehn for providing *Nodal*$^{fl/fl}$ mice, A. Yap, R. Krumlauf and P. Tam for comments on the manuscript, and T. Davidson for mouse colony maintenance. Confocal microscopy was performed at the Australian Cancer Research Foundation Dynamic Imaging Centre of Cancer Biology. Flow cytometry was performed with the assistance of the Queensland Brain Institute Flow Cytometry facility.

Funding
This work was supported by the National Health and Medical Research Council [APP1030146 to J.B.], the Australian Research Council [DP110105459 to J.B. and P.K.] and the Queensland Cancer Council [APP1012325 to J.B.].

Competing interests statement
The authors declare no competing financial interests.

Supplementary material
Supplementary material available online at
http://dev.biologists.org/lookup/suppl/doi:10.1242/dev.083006/-/DC1

References

Alberio, R., Croxall, N. and Allegrucci, C. (2010). Pig epiblast stem cells depend on activin/nodal signaling for pluripotency and self-renewal. *Stem Cells Dev.* **19**, 1627-1636.
Baldassarre, G., Romano, A., Armenante, F., Rambaldi, M., Paoletti, I., Sandomenico, C., Pepe, S., Staibano, S., Salvatore, G., De Rosa, G. et al. (1997). Expression of teratocarcinoma-derived growth factor-1 (TDGF-1) in testis germ cell tumors and its effects on growth and differentiation of embryonal carcinoma cell line NTERA2/D1. *Oncogene* **15**, 927-936.
Barrios, F., Filipponi, D., Pellegrini, M., Paronetto, M. P., Di Siena, S., Geremia, R., Rossi, P., De Felici, M., Jannini, E. A. and Dolci, S. (2010). Opposing effects of retinoic acid and FGF9 on Nanos2 expression and meiotic entry of mouse germ cells. *J. Cell Sci.* **123**, 871-880.
Bianco, C., Strizzi, L., Ebert, A., Chang, C., Rehman, A., Normanno, N., Guedez, L., Salloum, R., Ginsburg, E., Sun, Y. et al. (2005). Role of human cripto-1 in tumor angiogenesis. *J. Natl. Cancer Inst.* **97**, 132-141.
Bianco, C., Rangel, M. C., Castro, N. P., Nagaoka, T., Rollman, K., Gonzales, M. and Salomon, D. S. (2010). Role of Cripto-1 in stem cell maintenance and malignant progression. *Am. J. Pathol.* **177**, 532-540.
Bowles, J., Knight, D., Smith, C., Wilhelm, D., Richman, J., Mamiya, S., Yashiro, K., Chawengsaksophak, K., Wilson, M. J., Rossant, J. et al. (2006). Retinoid signaling determines germ cell fate in mice. *Science* **312**, 596-600.
Bowles, J., Feng, C. W., Spiller, C., Davidson, T. L., Jackson, A. and Koopman, P. (2010). FGF9 suppresses meiosis and promotes male germ cell fate in mice. *Dev. Cell* **19**, 440-449.
Brennan, J., Lu, C. C., Norris, D. P., Rodriguez, T. A., Beddington, R. S. and Robertson, E. J. (2001). Nodal signalling in the epiblast patterns the early mouse embryo. *Nature* **411**, 965-969.
Brons, I. G., Smithers, L. E., Trotter, M. W., Rugg-Gunn, P., Sun, B., Chuva de Sousa Lopes, S. M., Howlett, S. K., Clarkson, A., Ahrlund-Richter, L., Pedersen, R. A. et al. (2007). Derivation of pluripotent epiblast stem cells from mammalian embryos. *Nature* **448**, 191-195.
Buehr, M., McLaren, A., Bartley, A. and Darling, S. (1993). Proliferation and migration of primordial germ cells in We/We mouse embryos. *Dev. Dyn.* **198**, 182-189.
Camus, A., Perea-Gomez, A., Moreau, A. and Collignon, J. (2006). Absence of Nodal signaling promotes precocious neural differentiation in the mouse embryo. *Dev. Biol.* **295**, 743-755.
Ciccodicola, A., Dono, R., Obici, S., Simeone, A., Zollo, M. and Persico, M. G. (1989). Molecular characterization of a gene of the 'EGF family' expressed in undifferentiated human NTERA2 teratocarcinoma cells. *EMBO J.* **8**, 1987-1991.
Colvin, J. S., Green, R. P., Schmahl, J., Capel, B. and Ornitz, D. M. (2001). Male-to-female sex reversal in mice lacking fibroblast growth factor 9. *Cell* **104**, 875-889.
de Jong, J., Stoop, H., Gillis, A. J., van Gurp, R. J., van de Geijn, G. J., Boer, M., Hersmus, R., Saunders, P. T., Anderson, R. A., Oosterhuis, J. W. et al. (2008). Differential expression of SOX17 and SOX2 in germ cells and stem cells has biological and clinical implications. *J. Pathol.* **215**, 21-30.
DiNapoli, L., Batchvarov, J. and Capel, B. (2006). FGF9 promotes survival of germ cells in the fetal testis. *Development* **133**, 1519-1527.
Durcova-Hills, G. and Surani, A. (2008). Reprogramming primordial germ cells (PGC) to embryonic germ (EG) cells, *Curr. Protoc. Stem Cell Biol.* **2008**, Chapter 1: Unit 1A.3.
Durcova-Hills, G., Adams, I. R., Barton, S. C., Surani, M. A. and McLaren, A. (2006). The role of exogenous fibroblast growth factor-2 on the reprogramming of primordial germ cells into pluripotent stem cells. *Stem Cells* **24**, 1441-1449.
Gillis, A. J., Stoop, H., Biermann, K., van Gurp, R. J., Swartzman, E., Cribbes, S., Ferlinz, A., Shannon, M., Oosterhuis, J. W. and Looijenga, L. H. (2011). Expression and interdependencies of pluripotency factors LIN28, OCT3/4, NANOG and SOX2 in human testicular germ cells and tumours of the testis. *Int. J. Androl.* **34**, e160-e174.
Gray, P. C., Harrison, C. A. and Vale, W. (2003). Cripto forms a complex with activin and type II activin receptors and can block activin signaling. *Proc. Natl. Acad. Sci. USA* **100**, 5193-5198.
Gray, P. C., Shani, G., Aung, K., Kelber, J. and Vale, W. (2006). Cripto binds transforming growth factor beta (TGF-beta) and inhibits TGF-beta signaling. *Mol. Cell. Biol.* **26**, 9268-9278.
Guzman-Ayala, M., Ben-Haim, N., Beck, S. and Constam, D. B. (2004). Nodal protein processing and fibroblast growth factor 4 synergize to maintain a trophoblast stem cell microenvironment. *Proc. Natl. Acad. Sci. USA* **101**, 15656-15660.
Hammond, S. S. and Matin, A. (2009). Tools for the genetic analysis of germ cells. *Genesis* **47**, 617-627.
Holt, J. E., Jackson, A., Roman, S. D., Aitken, R. J., Koopman, P. and McLaughlin, E. A. (2006). CXCR4/SDF1 interaction inhibits the primordial to primary follicle transition in the neonatal mouse ovary. *Dev. Biol.* **293**, 449-460.
Honda, A., Hirose, M. and Ogura, A. (2009). Basic FGF and Activin/Nodal but not LIF signaling sustain undifferentiated status of rabbit embryonic stem cells. *Exp. Cell Res.* **315**, 2033-2042.
James, D., Levine, A. J., Besser, D. and Hemmati-Brivanlou, A. (2005). TGFbeta/activin/nodal signaling is necessary for the maintenance of pluripotency in human embryonic stem cells. *Development* **132**, 1273-1282.
Kehler, J., Tolkunova, E., Koschorz, B., Pesce, M., Gentile, L., Boiani, M., Lomelí, H., Nagy, A., McLaughlin, K. J., Schöler, H. R. et al. (2004). Oct4 is required for primordial germ cell survival. *EMBO Rep.* **5**, 1078-1083.
Kelly, R. K., Olson, D. L., Sun, Y., Wen, D., Wortham, K. A., Antognetti, G., Cheung, A. E., Orozco, O. E., Yang, L., Bailly, V. et al. (2011). An antibody-cytotoxic conjugate, BIIB015, is a new targeted therapy for Cripto positive tumours. *Eur. J. Cancer* **47**, 1736-1746.
Koubova, J., Menke, D. B., Zhou, Q., Capel, B., Griswold, M. D. and Page, D. C. (2006). Retinoic acid regulates sex-specific timing of meiotic initiation in mice. *Proc. Natl. Acad. Sci. USA* **103**, 2474-2479.
Lomelí, H., Ramos-Mejía, V., Gertsenstein, M., Lobe, C. G. and Nagy, A. (2000). Targeted insertion of Cre recombinase into the TNAP gene: excision in primordial germ cells. *Genesis* **26**, 116-117.
Looijenga, L. H. (2009). Human testicular (non)seminomatous germ cell tumours: the clinical implications of recent pathobiological insights. *J. Pathol.* **218**, 146-162.
Looijenga, L. H. and Oosterhuis, J. W. (1999). Pathogenesis of testicular germ cell tumours. *Rev. Reprod.* **4**, 90-100.
Looijenga, L. H., Stoop, H., de Leeuw, H. P., de Gouveia Brazao, C. A., Gillis, A. J., van Roozendaal, K. E., van Zoelen, E. J., Weber, R. F., Wolffenbuttel, K. P., van Dekken, H. et al. (2003). POU5F1 (OCT3/4) identifies cells with pluripotent potential in human germ cell tumors. *Cancer Res.* **63**, 2244-2250.
Looijenga, L. H., Gillis, A. J., Stoop, H., Biermann, K. and Oosterhuis, J. W. (2011). Dissecting the molecular pathways of (testicular) germ cell tumour pathogenesis; from initiation to treatment-resistance. *Int. J. Androl.* **34**, e234-e251.
Lowe, L. A., Yamada, S. and Kuehn, M. R. (2001). Genetic dissection of nodal function in patterning the mouse embryo. *Development* **128**, 1831-1843.
Matsui, Y. and Tokitake, Y. (2009). Primordial germ cells contain subpopulations that have greater ability to develop into pluripotential stem cells. *Dev. Growth Differ.* **51**, 657-667.
Matsui, Y., Zsebo, K. and Hogan, B. L. (1992). Derivation of pluripotential embryonic stem cells from murine primordial germ cells in culture. *Cell* **70**, 841-847.
McLaren, A. (1983). Primordial germ cells in mice. *Bibl. Anat.* **24**, 59-66.
Mendis, S. H., Meachem, S. J., Sarraj, M. A. and Loveland, K. L. (2011). Activin A balances sertoli and germ cell proliferation in the fetal mouse testis. *Biol. Reprod.* **84**, 379-391.
Mesnard, D., Guzman-Ayala, M. and Constam, D. B. (2006). Nodal specifies embryonic visceral endoderm and sustains pluripotent cells in the epiblast before overt axial patterning. *Development* **133**, 2497-2505.
Mithraprabhu, S., Mendis, S., Meachem, S. J., Tubino, L., Matzuk, M. M., Brown, C. W. and Loveland, K. L. (2010). Activin bioactivity affects germ cell differentiation in the postnatal mouse testis in vivo. *Biol. Reprod.* **82**, 980-90.
Monk, M. and McLaren, A. (1981). X-chromosome activity in foetal germ cells of the mouse. *J. Embryol. Exp. Morphol.* **63**, 75-84.

Moreno, S. G., Attali, M., Allemand, I., Messiaen, S., Fouchet, P., Coffigny, H., Romeo, P. H. and Habert, R. (2010). TGFbeta signaling in male germ cells regulates gonocyte quiescence and fertility in mice. *Dev. Biol.* **342**, 74-84.
Mosselman, S., Looijenga, L. H., Gillis, A. J., van Rooijen, M. A., Kraft, H. J., van Zoelen, E. J. and Oosterhuis, J. W. (1996). Aberrant platelet-derived growth factor alpha-receptor transcript as a diagnostic marker for early human germ cell tumors of the adult testis. *Proc. Natl. Acad. Sci. USA* **93**, 2884-2888.
Oosterhuis, J. W. and Looijenga, L. H. (2005). Testicular germ-cell tumours in a broader perspective. *Nat. Rev. Cancer* **5**, 210-222.
Postovit, L. M., Margaryan, N. V., Seftor, E. A., Kirschmann, D. A., Lipavsky, A., Wheaton, W. W., Abbott, D. E., Seftor, R. E. and Hendrix, M. J. (2008). Human embryonic stem cell microenvironment suppresses the tumorigenic phenotype of aggressive cancer cells. *Proc. Natl. Acad. Sci. USA* **105**, 4329-4334.
Resnick, J. L., Bixler, L. S., Cheng, L. and Donovan, P. J. (1992). Long-term proliferation of mouse primordial germ cells in culture. *Nature* **359**, 550-551.
Schier, A. F. (2003). Nodal signaling in vertebrate development. *Annu. Rev. Cell Dev. Biol.* **19**, 589-621.
Schier, A. F. (2009). Nodal morphogens. *Cold Spring Harb. Perspect. Biol.* **1**, a003459.
Shen, M. M. (2007). Nodal signaling: developmental roles and regulation. *Development* **134**, 1023-1034.
Skakkebæk, N. E., Berthelsen, J. G., Giwercman, A. and Müller, J. (1987). Carcinoma-in-situ of the testis: possible origin from gonocytes and precursor of all types of germ cell tumours except spermatocytoma. *Int. J. Androl.* **10**, 19-28.
Souquet, B., Tourpin, S., Messiaen, S., Moison, D., Habert, R. and Livera, G. (2012). Nodal signaling regulates the entry into meiosis in fetal germ cells. *Endocrinology* **153**, 2466-2473.
Speed, R. M. (1982). Meiosis in the foetal mouse ovary. I. An analysis at the light microscope level using surface-spreading. *Chromosoma* **85**, 427-437.
Strizzi, L., Bianco, C., Normanno, N. and Salomon, D. (2005). Cripto-1: a multifunctional modulator during embryogenesis and oncogenesis. *Oncogene* **24**, 5731-5741.
Suzuki, A. and Saga, Y. (2008). Nanos2 suppresses meiosis and promotes male germ cell differentiation. *Genes Dev.* **22**, 430-435.
Szabó, P. E., Hübner, K., Schöler, H. and Mann, J. R. (2002). Allele-specific expression of imprinted genes in mouse migratory primordial germ cells. *Mech. Dev.* **115**, 157-160.
Tesar, P. J., Chenoweth, J. G., Brook, F. A., Davies, T. J., Evans, E. P., Mack, D. L., Gardner, R. L. and McKay, R. D. (2007). New cell lines from mouse epiblast share defining features with human embryonic stem cells. *Nature* **448**, 196-199.
Tsuda, M., Sasaoka, Y., Kiso, M., Abe, K., Haraguchi, S., Kobayashi, S. and Saga, Y. (2003). Conserved role of nanos proteins in germ cell development. *Science* **301**, 1239-1241.
Vallier, L., Alexander, M. and Pedersen, R. A. (2005). Activin/Nodal and FGF pathways cooperate to maintain pluripotency of human embryonic stem cells. *J. Cell Sci.* **118**, 4495-4509.
van den Bergen, J. A., Miles, D. C., Sinclair, A. H. and Western, P. S. (2009). Normalizing gene expression levels in mouse fetal germ cells. *Biol. Reprod.* **81**, 362-370.
Watanabe, K., Meyer, M. J., Strizzi, L., Lee, J. M., Gonzales, M., Bianco, C., Nagaoka, T., Farid, S. S., Margaryan, N., Hendrix, M. J. et al. (2010). Cripto-1 is a cell surface marker for a tumorigenic, undifferentiated subpopulation in human embryonal carcinoma cells. *Stem Cells* **28**, 1303-1314.
Wechselberger, C., Strizzi, L., Kenney, N., Hirota, M., Sun, Y., Ebert, A., Orozco, O., Bianco, C., Khan, N. I., Wallace-Jones, B. et al. (2005). Human Cripto-1 overexpression in the mouse mammary gland results in the development of hyperplasia and adenocarcinoma. *Oncogene* **24**, 4094-4105.

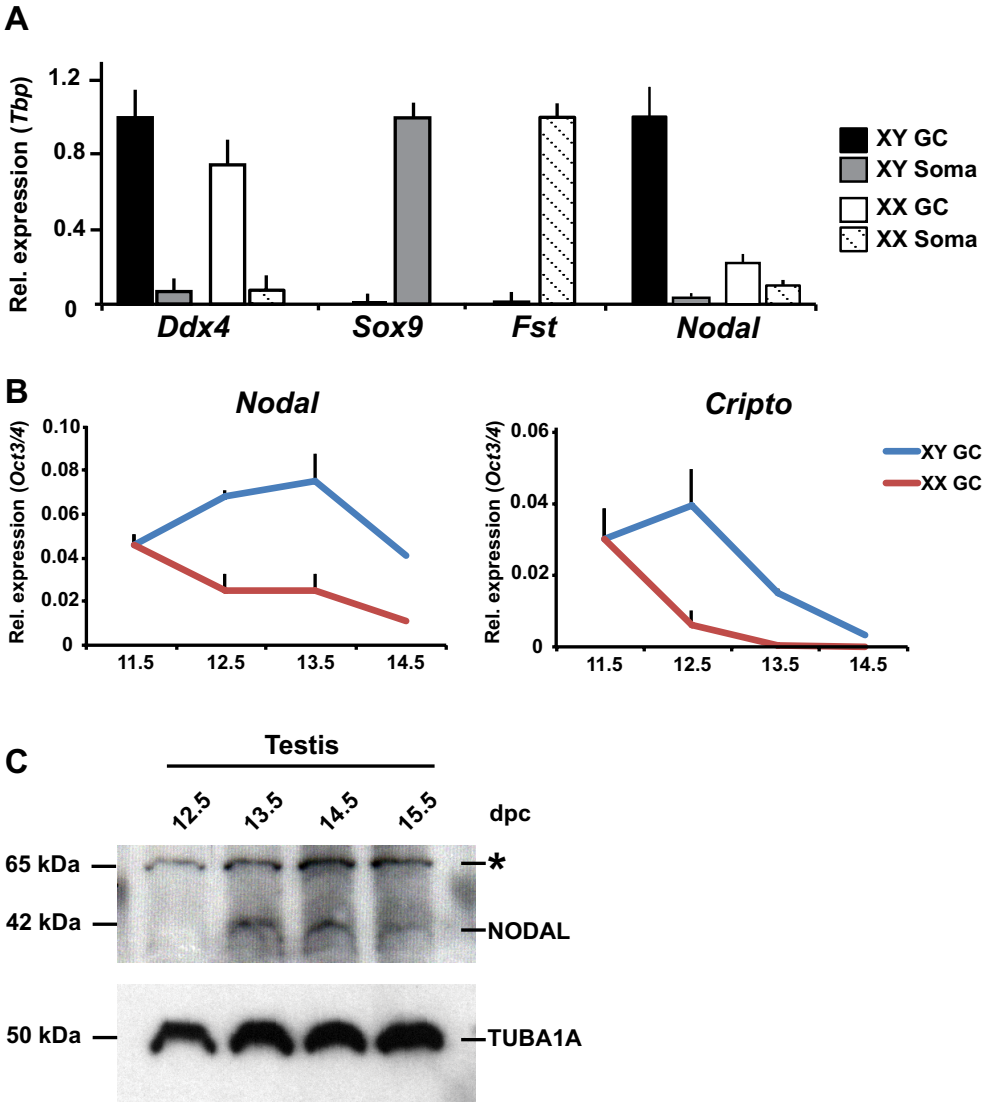

Fig. S1. Nodal pathway analysis in isolated germ cell populations and whole testes. (**A**) Expression of germ cell marker (*Ddx4*), somatic cell markers (*Sox9/Fst*) and *Nodal* in 13.5 dpc XY and XX germ and somatic cell populations isolated by FACS. *Ddx4* is detected at the highest level in germ cells and at low levels in somatic cell populations. XY Somatic marker *Sox9* (XY) and *Fst* (XX) are detected at highest levels in XY and XX somatic populations, respectively. *Nodal* is predominantly expressed in XY germ cells. Expression was normalized to *Tbp* and highest gene expression was set to 1; error bars represent s.e.m. of three independent isolations, each performed in triplicate. (**B**) Expression of *Nodal* and *Cripto* in XX and XY purified germ cell populations from 11.5-14.5 dpc isolated by FACS. Peak *Nodal* and *Cripto* expression was detected in XY germ cells at 13.5 and 12.5 dpc, respectively. (**C**) NODAL (42 kDa) was detected by western blot in XY gonad-only samples from 13.5 to 15.5 dpc. An additional band at 65 kDa (*) was detected using this antibody in all samples (12.5-15.5 dpc). TUBA1A was used as the loading control.

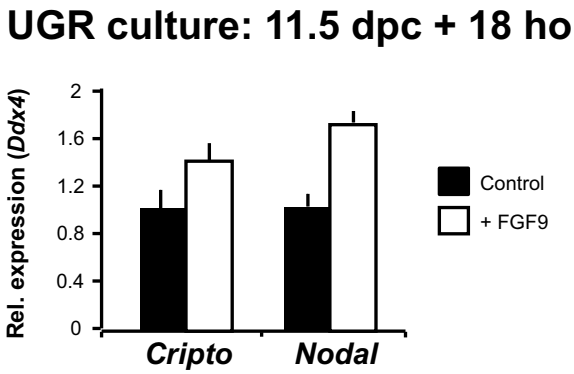

Fig. S2. FGF9 induces *Cripto* and *Nodal* expression in UGR culture. FGF9 induces both *Cripto* and *Nodal* expression in 11.5 dpc XY urogenital ridges cultured for 18 hours. Expression was normalised to *Ddx4* and control gene expression was set to 1. Error bars represent s.d. of technical replicates for one representative experiment.

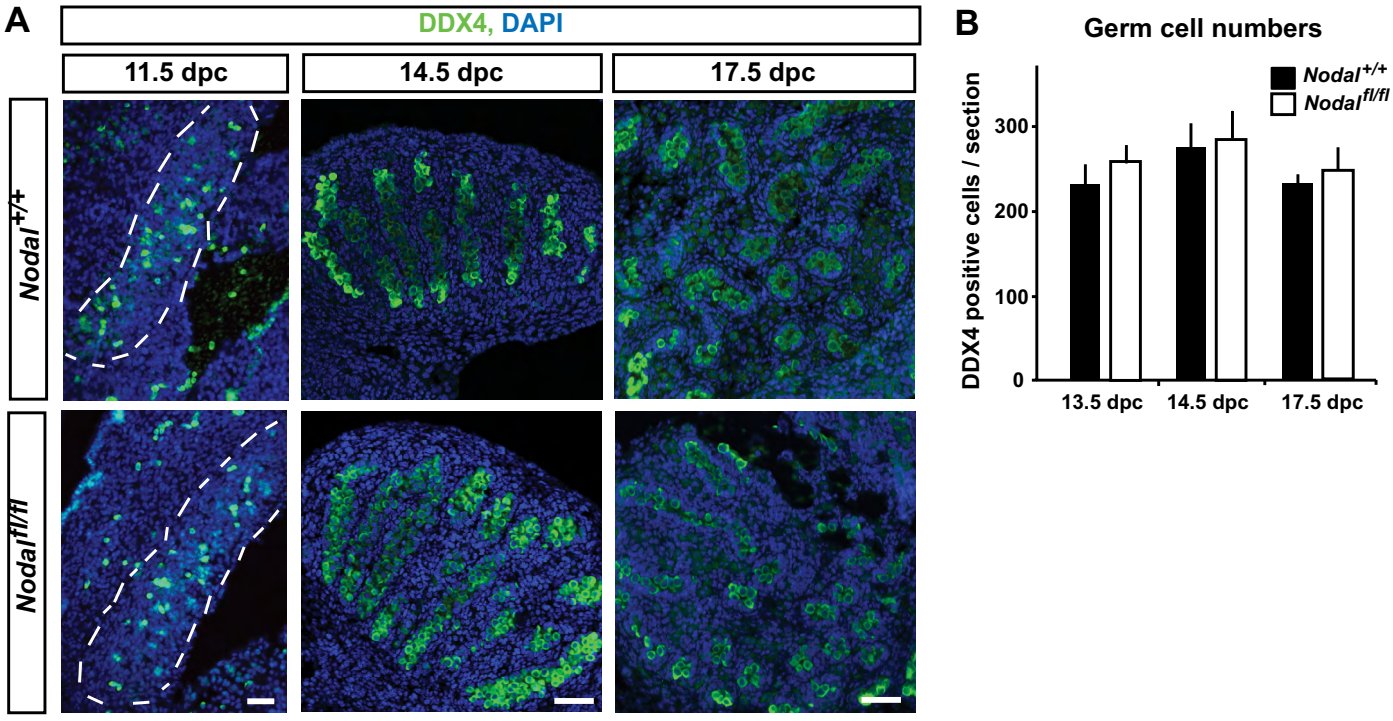

Fig. S3. Analysis of germ cell numbers in *Nodal*$^{fl/fl}$ mutants. (**A**) Germ cell marker DDX4 expression was detected in 11.5, 14.5 and 17.5 dpc XY *Nodal*$^{+/+}$, and *Nodal*$^{fl/fl}$ gonads. Nuclei are counterstained with DAPI. Scale bars: 100μm. (**B**) Quantification of total DDX4-positive cells (germ cells) per section in *Nodal*$^{+/+}$ and *Nodal*$^{fl/fl}$ gonads at 13.5, 14.5 and 17.5 dpc showed no significant difference in total germ cell number across genotypes at either timepoint.

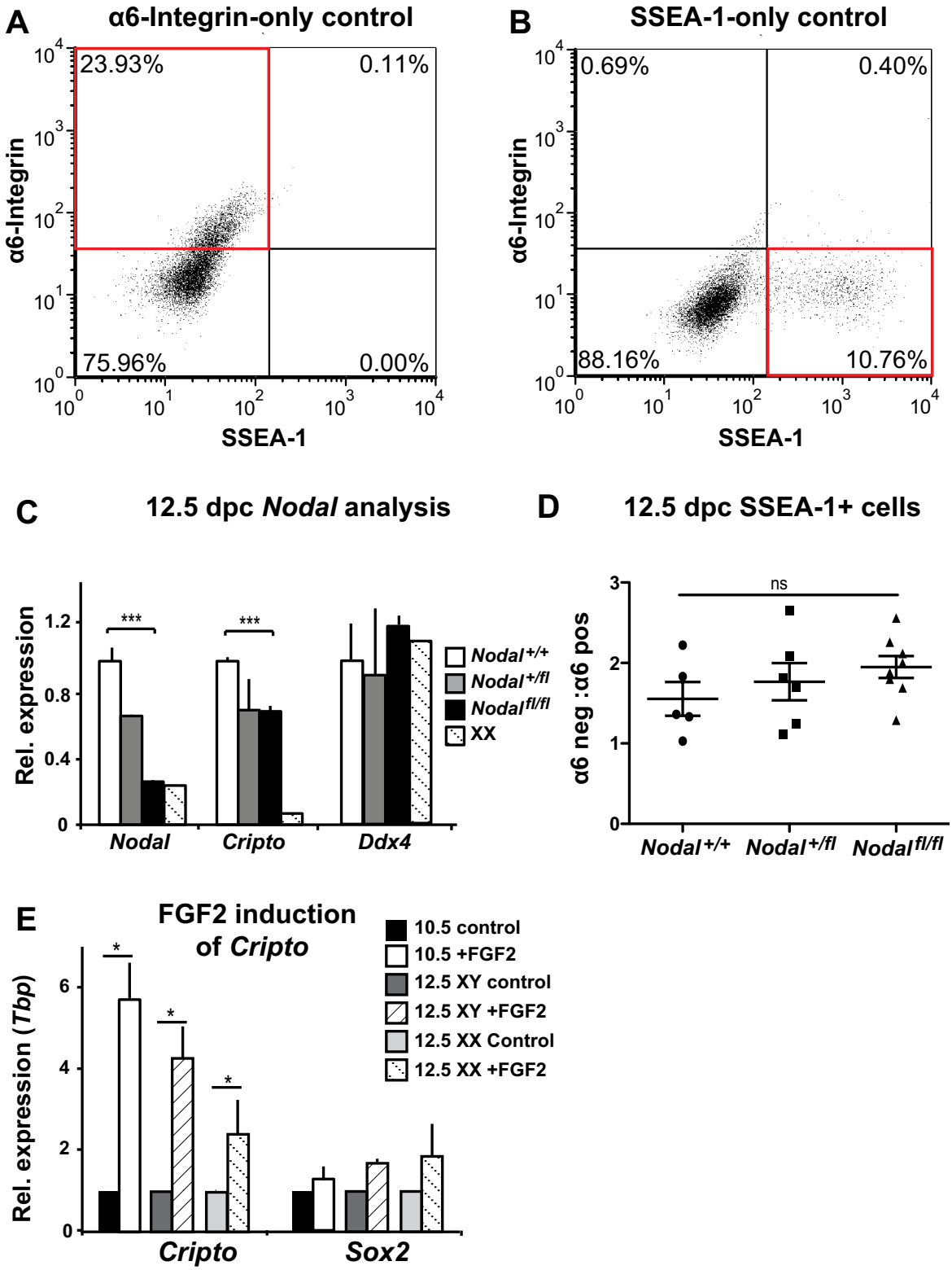

Fig. S4. *Nodal* expression is reduced in 12.5 dpc *Nodal*$^{fl/fl}$ gonads and FGF2 induces *Cripto* expression in isolated germ cells. (**A**,**B**) Single antibody controls for germ cell isolation using FACS: α6-integrin (A) and SSEA-1 (B). (**C**) *Nodal* and *Cripto* expression is decreased to ~20% and 70% of wild-type levels, respectively, in 12.5 dpc XY *Nodal*$^{fl/fl}$ gonads; *Ddx4* expression is not significantly altered across genotypes. Expression normalized to *Ddx4* (*Nodal* and *Cripto*) and *Tbp* (*Ddx4*), and wild-type gene expression was set to 1; *n*=3, 3, 3 and 2. (**D**) Using flow cytometry, ratios of α6-integrin-negative to α6-integrin-positive (SSEA-1-positive) germ cells were assessed as unchanged between Nodal genotypes at 12.5 dpc; *n*=5, 6 and 7. (**E**) Expression of *Sox2,* but especially *Cripto,* was induced in 10.5 dpc unsexed, and 12.5 dpc XY and XX isolated germ cells treated for 24 hours in the presence of FGF2 (25 ng/ml); *n*=3. Relative fold induction of *Cripto* by FGF2 was greatest in 10.5 dpc germ cells and lowest in 12.5 dpc XX germ cells, correlating precisely with the observed relative EG-forming efficiency of these populations. Expression normalized to *Tbp* and control group gene expression was set to 1. Error bars in C and D represent s.e.m.; statistical significance was assessed using Student's *t*-test (C,E) and one-way ANOVA (D); **P*<0.05; ****P*<0.0005. ns, not significant.

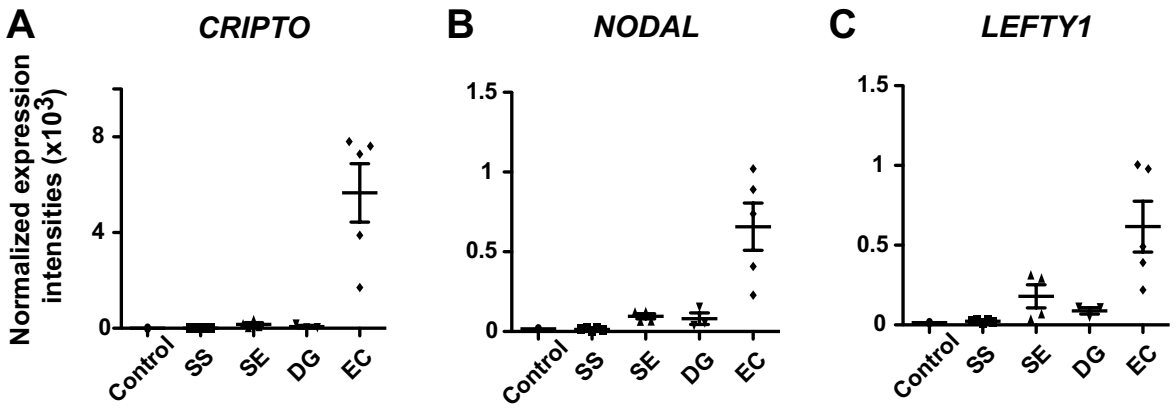

Fig. S5. *CRIPTO, NODAL* and *LEFTY1* expression are associated with embryonal carcinoma. Normalized expression intensities of *CRIPTO* (**A**), *NODAL* (**B**) and *LEFTY1* (**C**) from expression microarray analysis of three non-invasive tumour types: spermatocytic seminoma (SS), seminoma (SE) and dysgerminoma (DG), compared with the invasive non-seminoma tumour embryonal carcinoma (EC); *n*=5, 4, 3 and 5. Data are mean±s.e.m.

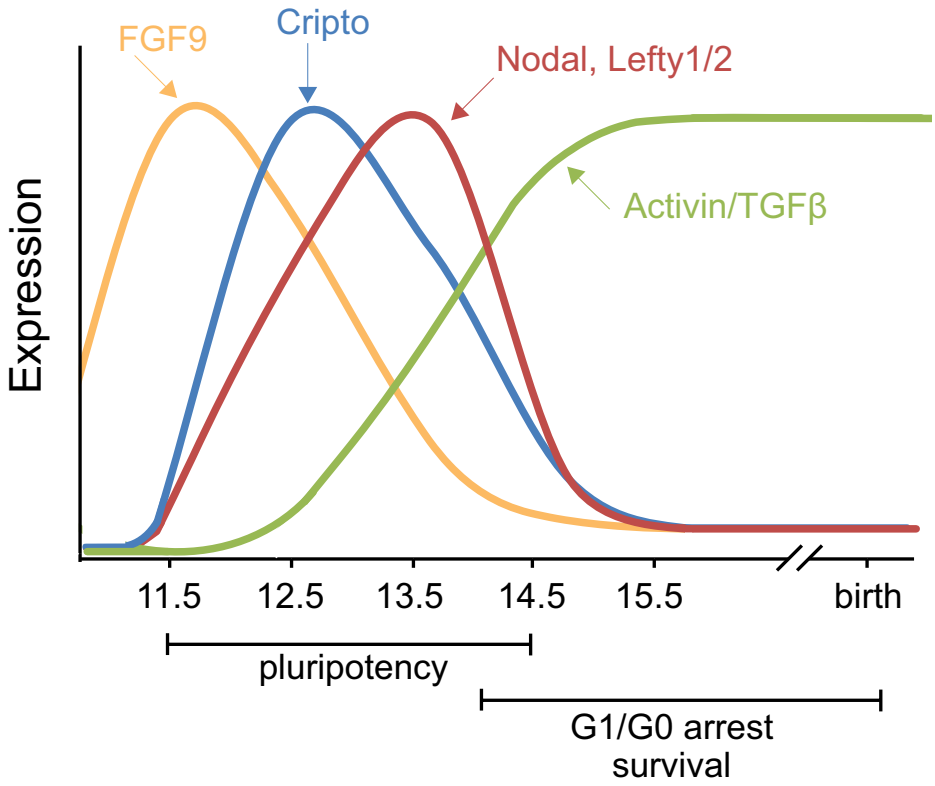

Fig. S6. Expression of Fgf9, Nodal and activin/TGFβ members during XY germ cell development. Fgf9 is expressed by the somatic cells of the testis with expression peaking around 11.5 dpc, prior to sex differentiation of the germ cells. Fgf9 expression increases *Cripto* expression in XY germ cells, which peaks at 12.5 dpc. The expression of Cripto on germ cells allows autocrine Nodal signaling to induce expression of itself and downstream targets *Lefty1* and *Lefty2*, which display peak expression at 13.5 dpc. Expression of *Nodal* and *Cripto* at this time serves to maintain pluripotency in the XY germ cell population as in its absence, pluripotency potential of the germ cells is reduced. By 14.5 dpc expression of activin and its receptors is present throughout the whole gonad, peaking at 16.5 dpc, and plays a role in germ cell G1/G0 arrest and survival (Mithraprabhu et al., 2010; Moreno et al., 2010; Mendis et al., 2011).

Table S1. Taqman probe sets and Sybr primer details used for real time qRT-PCR

Gene	Taqman (human)	Taqman (mouse)	SYBR Fwd primer (5'-3')	SYBR Rev primer (5'-3')
HPRT	Hs01003267_m1			
Sdha		Mm01352366_m1		
Tbp	Hs00427621_m1	Mm00446973_m1	ACGGACAACTGCGTTGATTTT	ACTTAGCTGGGAAGCCCAAC
Nodal	Hs00415443_m1	Mm00443040_m1	CATGTTGAGCCTCTACCGAGAC	CGTGAAAGTCCAGTTCTGTCCG
Cripto/Tdgf1	Hs02339499_g1	Mm00783944_g1	CGTCAGAAGATGGGGTACTTC	ACGGGTCCAAATTCAAACAC
Lefty1	Hs00764128_s1	Mm00438615_m1	GAGGCAAGAGGTTCAGCCAGAA	CGCTGCTCCATTCCGAACACTA
Lefty2		Mm00774547_m1	ACACGCTGGACCTCAAGGACTA	GTACATCTCCTGGCGACAGCAT
Ddx4		Mm00802445_m1		
Nanog		Mm02019550_s1		
Oct4/Pou5f1		Mm00658129_gH		
Sox2		Mm00488369_s1		
Sox9		Mm00448840_m1		
Fst		Mm00514982_m1		
Nanos2		Mm02525720_s1		
Dnmt3L		Mm00457635_m1		
P15/Cdkn2b		Mm00483241_m1		
Stra8		Mm00488519_m1		
18S rRNA			GATCCATTGGAGGGCAAGTCT	CCAAGATCCAACTACGAGCTTTTT
ActRIIB			GGAAGGCTCAGCTCATGAACGA	TGCCGGGTGTGCTGAAGATTTC
Alk4			AGAGGGTGGGGACCAAAC	TGCTTCATGTTGATTGTCTCG
Alk7			ACACTGCACCTTCCCACAG	AATTGTCCTTGCGATTGTTCTT